Heterogeneous Fenton-like degradation of EDTA in an aqueous solution with enhanced COD removal under neutral pH

Junfeng Hua and Mei Huang

ABSTRACT

By providing the key carbon and nitrogen elements needed for eutrophication, the potential toxicity of ethylenediaminetetraacetic acid (EDTA) prompts the exploration of effective treatment methods to minimize the amount of EDTA released into the environment. In this study, Fe_3O_4 magnetic nanoparticles (MNPs) were prepared and used as catalysts to study the mineralization of EDTA in Fenton-like reactions under neutral pH. Fe_3O_4 MNPs were characterized by X-ray diffraction (XRD), transmission electron microscopy (TEM), and Brunauer–Emmett–Teller (BET). The effects of pH, ferric ion leaching, and H_2O_2 concentration on chemical oxygen demand (COD) removal of EDTA were investigated. The morphological characterization of the nanoparticles suggests a quasi-spherical structure with small particle size and a surface area of 49.9 m^2/g. The results show that Fe_3O_4 MNPs had good catalytic activity for the mineralization of EDTA under pH 5.0–9.0. The optimum conditions for the COD removal of 45% at pH 7.0 were: 40 mM H_2O_2, 10 mM Fe_3O_4, and 1 g/L EDTANa$_2$·2H$_2$O at 303 K. Fe_3O_4 MNPs maintained high catalytic activity after five cycles of continuous degradation of EDTA. According to reactive oxidizing species measurements obtained by electron spin resonance (ESR), it was confirmed that HO· free radicals, presented in the H_2O_2/Fe_3O_4 MNPs heterogeneous Fenton-like reaction, were the primary active group in the removal of EDTA. These features can be considered beneficial to the application of Fe_3O_4 MNPs towards industrial wastewater treatment.

Key words | COD, EDTA mineralization, Fe_3O_4 MNPs, heterogeneous Fenton-like reaction, hydroxyl radicals, neutral pH

Junfeng Hua
Mei Huang (corresponding author)
College of Chemical & Biochemical Engineering,
Zhejiang University,
Zheda Road, Hangzhou 310027,
China
E-mail: huangm@zju.edu.cn

Mei Huang
Institute of Zhejiang University – Quzhou,
78 Jiuhua Boulevard North, Quzhou 324000,
China

HIGHLIGHTS

- Fe_3O_4 MNPs showed an enhanced COD removal rate of EDTA under neutral pH.
- Higher H_2O_2 oxidation efficiency was observed for EDTA degradation.
- Fe_3O_4 MNPs maintained high activity in five reaction cycles.
- HO· radicals existed in the H_2O_2/Fe_3O_4 MNPs heterogeneous Fenton-like reaction.

INTRODUCTION

Wastewater discharged from industrial and commercial sources, such as chemical industries, textile industries, and leather manufacturing, often contains considerable amounts of organic pollutants. These contaminants can negatively impact ecosystems and humans due to their toxic, carcinogenic or mutagenic properties (Bissey *et al.* 2006; Ndjou'ou *et al.* 2006; Lv *et al.* 2012). Therefore, the efficient degradation of organics from industrial wastewater before discharging is critical. In recent years, advanced oxidation process (AOP) has received considerable attention due to its high removal ability of recalcitrant organic contaminants in aqueous solutions (Gągola *et al.* 2018; Kanakaraju *et al.* 2018). The Fenton process, a well-known AOP, has been widely tested for various industrial wastewaters with

recalcitrant compounds. However, several drawbacks, such as high consumption of H_2O_2, the low-speed generation of Fe(II), and acidic reaction conditions (generally at pH = 3.0), hamper the large-scale application of Fenton reactions in environmental remediation (Zhu *et al.* 2019). Moreover, after treatment, wastewater must be neutralized before discharging; thus, a large amount of slurry is produced. Subsequently, it is increasingly difficult and costly to further treat solid waste (Zhang *et al.* 2019).

The use of Fenton-like reactions, which derive from ferric ions reacting with H_2O_2 to produce ferrous ions at a very slow rate, can be applied with a heterogeneous catalyst to overcome some of the above mentioned limitations. For example, introducing additional electrons to heterogeneous Fenton catalysts can accelerate the generation of Fe(II) (Zhu *et al.* 2019). In addition, the *in situ* generation of H_2O_2 can be obtained by combining ultrasound, electricity, semiconductors, and iron-based catalysts in the system (Chen & Wang 2019; Zárate-Guzmán *et al.* 2019), and controlling the specific morphologies and exposed facets of heterogeneous Fenton catalysts can greatly promote the decomposition of H_2O_2. Meanwhile, due to the supplementary recovery and recycling procedures, the amount of waste is largely reduced. In particular, it was found that Fenton-like catalysis can exhibit high activity in a wide pH range from neutral to alkaline conditions (Shi *et al.* 2020; Xia & Nan 2020). Among these heterogeneous catalysts, it has been reported that Fe_3O_4 nanoparticles have relatively high reactivity, in combination with H_2O_2, towards organic compounds in near-neutral conditions (Wang *et al.* 2015; Yang *et al.* 2015; Nascimentoa *et al.* 2019). Zhang reported that when the concentrations of Fe_3O_4 magnetic nanoparticles (MNPs) and H_2O_2 were 5 g/L and 1.2 M, respectively, phenol and aniline could be removed completely after 6 h of reaction at 308 K, and the total organic carbon (TOC) abatement efficiency for phenol and aniline were 42.79% and 40.38%, respectively (Zhang *et al.* 2009).

Ethylenediaminetetraacetic acid (EDTA) is a typical organic amine molecule with a high coordination character that is often used as a chelating agent in industrial processes (Madden *et al.* 1997; Chiang *et al.* 2004; Wang *et al.* 2012). However, when EDTA enters a body of water, its presence increases the chemical oxygen demand (COD). At the same time, EDTA can also provide key elemental nitrogen that leads to eutrophication of water bodies. Therefore, many efforts have been made to remove EDTA using advanced oxidation processes. Pirkanniemi *et al.* (2007) reported that over 90% of EDTA was degraded in water within 3 min at pH 4.0 and 60 °C. The molecular ratio of

$H_2O_2:Fe^{2+}$: EDTA was 70:2:1 (0.26 mM EDTA). Sillanpaa *et al.* (2009) used metallophthalocyanines as catalysts, in combination with H_2O_2, to remove 90% of EDTA within 3 h of reaction time. Despite these efforts, most of the previous studies have been focused on the degradation performance of EDTA without considering the mineralization extent and removal after the AOP. Since the total amount of C and N in the water remains after the Fenton-like reaction is achieved, the water treated can still have a negative impact in the environment after discharge if the total C and N are high. Therefore, instead of simple degradation, complete mineralization of EDTA from water can have a significant impact in understanding Fenton-like reactions for industrial wastewater treatment. In fact, due to the high water solubility of Na-EDTA and its low adsorption capacity to various adsorbents, as well as its poor mineralization, it is difficult to completely remove EDTA by conventional treatment methods (Yang *et al.* 2005; Sailo *et al.* 2015).

In order to prevent the conversion of EDTA into the key elements, carbon and nitrogen, that cause eutrophication in water during the degradation process, this study investigated the mineralization of EDTA using Fe_3O_4 MNPs as a catalyst in Fenton-like reactions under neutral pH. Although there are many studies that have applied Fe_3O_4 and H_2O_2 for decomplexation of metal-EDTA, their experimental results were accompanied by spontaneous increases in NH_4^+-N, inorganic carbon concentration and solution pH (Wang *et al.* 2020). In addition, a lot of work has been done on EDTA as a chelating agent to enhance the activation of H_2O_2 on the surface of Fe_3O_4 nanoparticles, thereby enhancing heterogeneous Fenton reactions by accelerating the formation of reactive oxygen species and increasing the degradation rates of various organic pollutants (He *et al.* 2015; Wang *et al.* 2017). However, there is little research on EDTA's own mineralization during the oxidation process. In this work, the effects of pH, ferric ion leaching, and H_2O_2 concentration on COD removal of EDTA were investigated thoroughly. In addition, the possible mechanism related to the mineralization of EDTA was also discussed.

MATERIALS AND METHODS

Reagents

All reagents used in the experiments were of at least analytical reagent grade and used without further purification. Hydrogen peroxide (H_2O_2) 30% (w/w), ferric chloride ($FeCl_3.6H_2O$), ferrous sulfate ($FeSO_4.7H_2O$), sodium sulfite

anhydrous (Na_2SO_3), ammonia ($NH_3 \cdot H_2O$; 25%, w/w), sulfuric acid (H_2SO_4) and sodium hydroxide (NaOH) were obtained from Beijing Chemicals Corporation (Beijing, China). Ethylenediaminetetraacetic acid disodium salt dihydrate ($EDTANa_2 \cdot 2H_2O$, 98.5%) and 5,5-Dimethyl-1-pyrroline N-oxide (DMPO) were purchased from Sigma-Aldrich Co., USA. Ultrapure water was supplied by Hangzhou Wahaha Group Co., Ltd (Hangzhou, China).

Magnetic catalyst preparation

Fe_3O_4 MNPs were prepared based on Massart's method by co-precipitation of Fe^{2+} and Fe^{3+} in an alkaline solution (Massart 1981). In a typical preparation procedure, 0.06 mol/L $FeCl_3$ and $FeSO_4$ solutions were mixed uniformly, and then a diluted ammonia solution was added dropwise. After vigorous stirring for 2 h under argon, black particles were deposited and separated from the solution by a powerful magnet. The particles were washed with deionized water and ethanol until the pH of the aqueous solution was neutral. Then, the particles were dried under vacuum and stored in a desiccator for further experiments.

Characterization of Fe_3O_4 MNPs

A crystallographic study was performed at room temperature on an X'Pert PRO X-ray diffractometer (XRD) with Cu-Kα radiation at 40 kV and 40 mA. The morphology and size distribution of Fe_3O_4 MNPs were observed with a CM200 transmission electron microscope (TEM). The Brunauer–Emmett–Teller (BET) surface area was examined using nitrogen adsorption–desorption isotherm measurements at 77 K on an ASAP 2020 surface area and porosity analyzer.

Experimental procedure and analytical methods

Before the experiments, 1,000 mL of EDTA solution with a predetermined concentration was prepared. The Fe_3O_4 MNPs catalyst was dispersed in 100 mL of $EDTANa_2 \cdot 2H_2O$ solution at an initial concentration of 1 g/L (COD of 616 ppm). The pH value of $EDTANa_2 \cdot 2H_2O$ solution was adjusted with solutions of H_2SO_4 or NaOH, respectively. Degradation of EDTA was initiated by rapidly adding a desired dosage of H_2O_2. The samples were agitated at room temperature at 250 rpm for 4 h. At selected time intervals, aliquots were withdrawn, and the catalyst was separated with a magnet. After appropriate Na_2SO_3 was added to quench excess H_2O_2, all samples were filtered through a 0.45 μm membrane and stored for subsequent analysis. Each experiment was

conducted in duplicate in 1 g/L $EDTANa_2 \cdot 2H_2O$ solution and the results obtained had error of less than 2%.

To recover Fe_3O_4 MNPs, the Fe_3O_4 MNPs used were magnetically separated with a magnet. The separated Fe_3O_4 MNPs were washed with deionized water followed by ethanol to resume the original state. After washing three times, the recovered Fe_3O_4 MNPs were dried and the catalytic activity was determined following the aforementioned protocol. Seven consecutive catalysis cycles were performed to test the reusability of the catalyst.

The COD was measured using a COD measurement kit (Hach DRB 200, DR 900 COD). The pH of the solution was measured with a PHS-3C pH-meter. Total leaching iron concentration was measured, according to the 1,10-phenanthroline method (Amonette & Templeton 1998), using a Lambda 25 UV/vis spectrophotometer (PerkinElmer) at 510 nm. Hydrogen peroxide concentration in the solution was determined by the iodometric titration method (Kavitha & Palanivelu 2004).

The electron spin resonance (ESR) spectra were obtained with a BRUKER ESRA-300 spectrometer at room temperature. The spectrometer parameters were as follows: scan range of 0–100 G; modulation frequency of 100 kHz; modulation amplitude of 1.0 G; time constant of 10.24 ms; conversion time of 20 ms; microwave power of 20.2 mW; and receiver gain of $3.99 \times 10E4$. DMPO was used to trap the free radicals during the reaction.

RESULTS AND DISCUSSION

Structural characterization of Fe_3O_4 MNPs

The crystalline structure of Fe_3O_4 MNPs was confirmed by XRD analysis. As seen from Figure 1, the diffraction peaks ({220}, {311}, {400}, {422}, {511} and {440}) could be indexed to the face-centered-cubic Fe_3O_4 (JCPDS no. 19–0629) (Zeng et al. 2010; Liu et al. 2011). Additionally, all Fe_3O_4 MNPs spectra were in good agreement with characteristic reflections centered at 36.2°. According to Scherrer's equation, the average particle size was calculated to be 20.8 nm for the prepared Fe_3O_4 MNPs. Because the precipitant used in the experiment was ammonia, the prepared Fe_3O_4 MNPs were slightly different from those obtained by other methods. For example, the classic Massart method uses tetramethylammonium hydroxide as an alkaline precipitant, so the average particle size of the prepared nanoparticles was 12 nm (Massart 1981). Moreover, when sodium hydroxide is used as a precipitant, it has been reported that the obtained
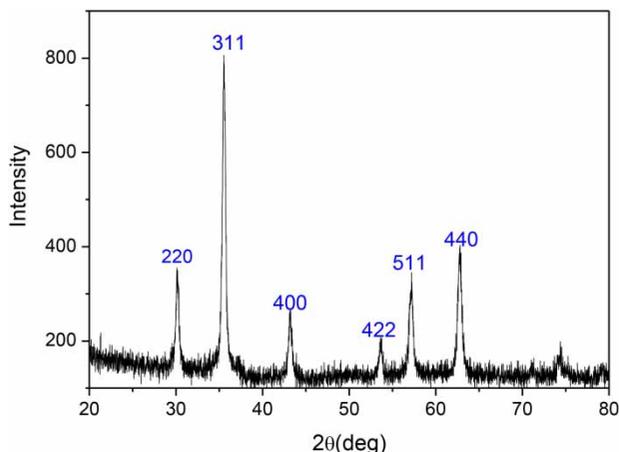
Figure 1 │ XRD pattern of Fe$_3$O$_4$ MNPs.

Fe$_3$O$_4$ MNPs were quasi-spherical with an average diameter of approximately 10 nm (Zhang *et al.* 2009).

The TEM images were also obtained to illustrate particle size and morphology of Fe$_3$O$_4$ MNPs. As shown in Figure 2, the prepared Fe$_3$O$_4$ MNPs were quasi-spherical with a uniform distribution of particle size. The average diameter of Fe$_3$O$_4$ was about 20 nm. This measurement agreed with the XRD observations.

Based on the BET method, the specific surface area of Fe$_3$O$_4$ MNPs was calculated to be 49.9 m^2/g. The average pore diameter was about 21.5 nm. As illustrated in Figure 3, the N$_2$ absorption/desorption isotherm for the Fe$_3$O$_4$ MNPs was proposed as IUPAC type IV with a hysteresis loop.

Effect of pH on EDTA mineralization

The influence of pH on the mineralization of EDTA was investigated over a wide pH range (3–11). Figure 4
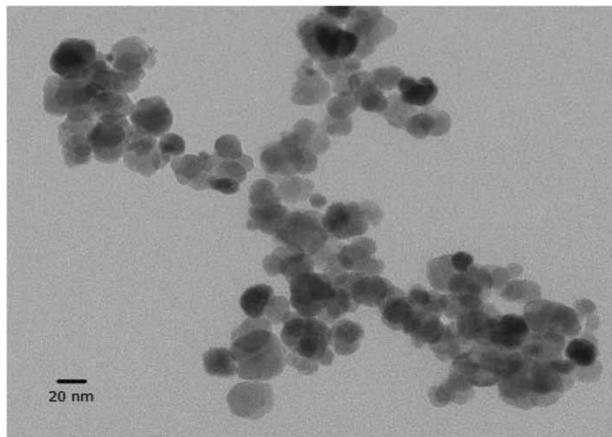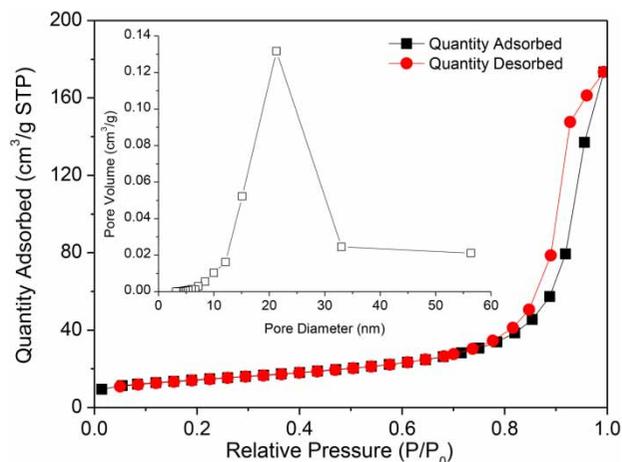

Figure 2 │ TEM image of Fe$_3$O$_4$ MNPs.

Figure 3 │ Nitrogen adsorption/desorption isotherms and pore size distribution (inset) of Fe$_3$O$_4$ MNPs.
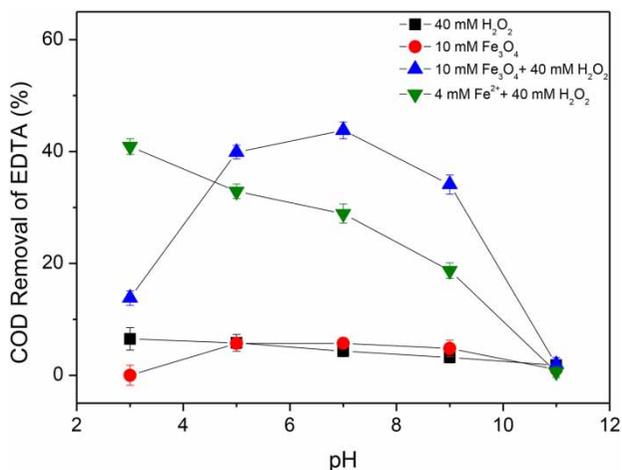

Figure 4 │ The COD removal of 1 g/L EDTANa$_2$·2H$_2$O at 303 K under different pH conditions and after 4 h (40 mM H$_2$O$_2$, 10 mM Fe$_3$O$_4$ MNPs).

shows the COD removal of EDTA when using H$_2$O$_2$ only, Fe$_3$O$_4$ MNPs only, and the combination of the magnetic catalyst and two concentrations of oxidant. When 40 mM H$_2$O$_2$ was used in the oxidation reaction, the COD removal rate of EDTA was less than 7% at all pH values tested. Compared with the oxidation potential of hydroxyl radicals, the limited removal efficiency might be due to the weak oxidation potential of H$_2$O$_2$ in the absence of a catalyst (Kwan & Voelker 2003). When Fe$_3$O$_4$ MNPs were used as the adsorbent for EDTA removal without adding any oxidizing agent, the COD removal rate of EDTA was less than 6% at all pH values tested. It was clear that Fe$_3$O$_4$ MNPs had limited adsorption capacity for EDTA removal in both acidic and alkaline conditions. Similar conclusions were obtained

in other studies that the adsorption capacity of EDTA on the adsorbents was small over a wide pH range (Wardas & Lebek 1998; Guo et al. 2013).

In the Fenton reaction system, the COD removal rate of EDTA reached a maximum of 40.9% for the following conditions: pH 3.0, 40 mM H_2O_2, and a ratio of H_2O_2 to Fe^{2+} of 10:1. When the pH of the solution was increased from 5.0 to 9.0, the removal efficiency of the Fenton reaction was reduced from 32.9% to 18.7%. These results demonstrated that the Fenton reaction could efficiently oxidize EDTA but only in a narrow acidic pH range.

When compared to the conventional Fenton reaction, Fe_3O_4 MNPs showed improved performance when increasing the pH of the solution. The COD removal rate of EDTA was 30–40% in the pH range of 5.0–9.0 and reached a maximum of 45% at pH 7.0. It is worth noting that the mineralization of EDTA significantly improved under neutral conditions, according to the enhanced catalytic performance of Fe_3O_4 MNPs.

The efficiency of the catalytic oxidation can be determined by comparing the adsorption of EDTA in the MNPs in the absence and presence of H_2O_2 at different pH values. The adsorption of EDTA, in terms of COD removal, was slightly higher at pH 7.0 compared to other pH values. In the presence of the oxidizing agent, the COD removal of EDTA achieved a maximum at 7.0. Considering the heterogeneity of the oxidation reaction, it was reasonable to consider that the effective adsorption of EDTA at the interface may contribute to the mineralization of EDTA. Through the synergistic action of adsorption and oxidation, the concentration of reactants at the interface increased, resulting in an enhancement in the efficiency of the oxidation reaction.

Effect of ferric ion leaching

In order to determine the role of ferric ions leached in solution during EDTA degradation with Fe_3O_4 MNPs, the determination of the concentration of ferric ions and residual H_2O_2 was studied in the pH range 3–11. The initial conditions were the following: 1 g/L of EDTANa$_2$·2H$_2$O, 40 mM H_2O_2 and 10 mM Fe_3O_4 MNPs. Figure 5 shows that both ferric ion leaching and H_2O_2 residual decreased with increasing pH. At pH 3.0, the residual H_2O_2 was 85% and the ferric iron leaching reached the maximum concentration of 18.9 mg/L. When the pH was 7.0, the COD removal of EDTA reached a maximum (see Figure 4) while the ferric ion concentration decreased to 0.6 mg/L.
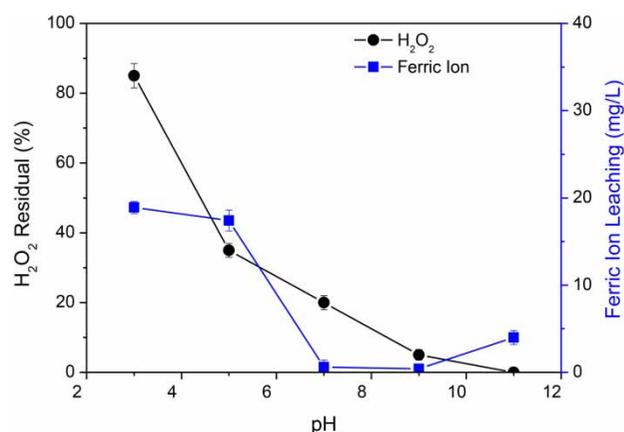

Figure 5 | Investigation of H_2O_2 residual and iron leaching with varied pH after 4 h (40 mM H_2O_2, 10 mM Fe_3O_4 and 1 g/L EDTA Na$_2$·2H$_2$O).

This suggests that there was no relationship between dissolved ferric ion and COD removal. In order to gain knowledge into the contribution of ferric ions to the oxidation reaction, additional experiments were conducted using 0.6 mg/L ferric ion to replace 10 mM Fe_3O_4 as the catalyst. Only a 5% COD removal of EDTA was found in the ferric ion solution at pH 7.0. This indicates that the degradation of EDTA mainly occurred on the surface of Fe_3O_4 MNPs, while the contribution of ferric ions to the catalytic degradation of EDTA was minimal. It can be seen that at pH = 7, the residual rate of H_2O_2 in the Fe_3O_4/H_2O_2 system was the smallest, while the COD removal of EDTA was the highest. The fact that high utilization rate of H_2O_2 was accompanied by the high mineralization of EDTA showed that the Fe_3O_4/H_2O_2 system can effectively remove EDTA under neutral conditions. The characteristic oxidation reaction condition not only eliminates the neutralization process required for wastewater treatment after the oxidation reaction, but also reduces the generation of solid sludge. It is of great significance for the usages of the Fe_3O_4/H_2O_2 system, which will provide potential benefits for the treatment of real-world wastewater.

Effect of Fe_3O_4 MNPs concentration on COD removal of EDTA

Figure 6 illustrates the effect of the concentration of Fe_3O_4 MNPs on the COD removal of EDTA. When the concentration of Fe_3O_4 MNPs increased from 1.25 to 10 mM, the COD removal rate increased from 28% to 45% at a fixed H_2O_2 dosage. The enhanced mineralization was attributed to the increased number of active sites on the surface of Fe_3O_4 MNPs. Therefore, more HO· free radicals could be
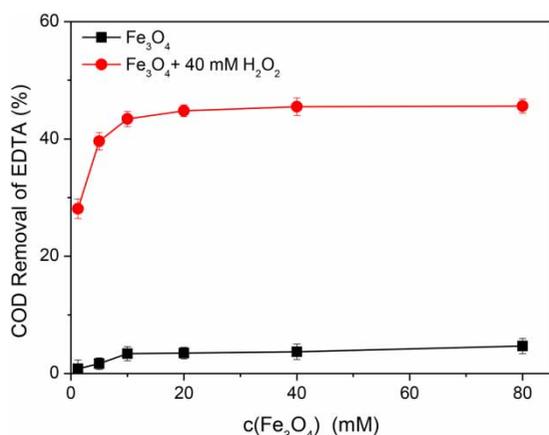
Figure 6 | Effect of Fe₃O₄ MNPs on COD removal efficiency of EDTA at pH 7 after 4 h (303 K 1 g/L EDTANa₂·2H₂O).

produced through accelerated reactions between H_2O_2 and Fe₃O₄ MNPs. Since the adsorption of EDTA on the Fe₃O₄ surface was less than 6%, it can be inferred that EDTA was mainly removed by Fenton-like heterogeneous oxidation, rather than by an adsorption process.

Effect of H_2O_2 dosage on COD removal of EDTA

Figure 7 shows the COD removal of EDTA under different H_2O_2 concentrations. The maximum COD removal rate was 45% at a H_2O_2 concentration of 40 mM. When the H_2O_2 concentration increased from 40 to 120 mM, no significant increase was observed in the COD removal of EDTA. These experimental results may be attributed to two different roles of hydrogen peroxide in the reaction. It is generally believed that the oxidation efficiency will increase with an increasing amount of oxidant added.
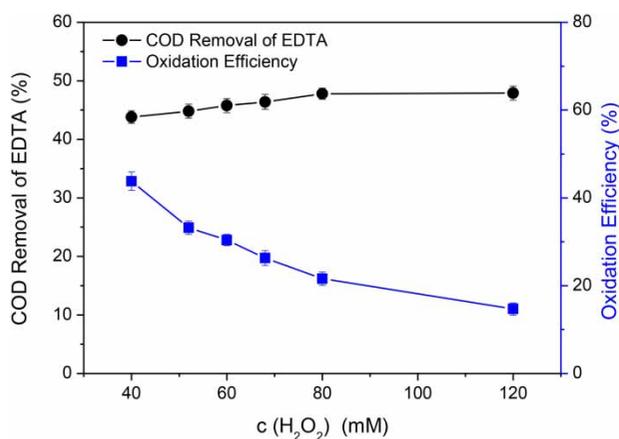

Figure 7 | Effect of H_2O_2 concentration on COD removal efficiency (1 g/L EDTANa₂·2H₂O, 10 mM Fe₃O₄, pH 7, 303 K, 4 h).

Then, the removal rate of EDTA should also increase with an increasing amount of H_2O_2. However, the fact that excess H_2O_2 will cause competition between different coexisting ions on the surface of Fe₃O₄ nanoparticles indicated that more H_2O_2 could weaken the adsorption of EDTA at the interface and reduce the oxidation reaction efficiency. Moreover, it is common to have a plateau of the EDTA removal rate in the oxidation reaction. Additionally, it has been reported that excess H_2O_2 can exist as a free radical scavenger (Olive *et al.* 2000; Madden & Taniguchi 2001). Therefore, when the H_2O_2 concentration is high, it is difficult to obtain an increased HO· radical concentration to oxidize EDTA. As shown by the experiments, when H_2O_2 concentration changed from 40 to 120 mM, the EDTA removal rate tended to stabilize.

However, it was also found in Figure 7 that the oxidation efficiency of H_2O_2 (Equation (1)) decreased with an increasing amount of H_2O_2 as follows:

$$Oxidation\,efficiency = \frac{COD_0 - COD_e}{16 \times C_0 V} \times 100 \qquad (1)$$

where COD_0 and COD_e represent the initial and final chemical oxygen demand (mg/L), respectively; V is the volume of the solution (mL); and C_0 is the concentration of H_2O_2 (mmol/mL).

Since the initial concentration of EDTA remained unchanged in all experiments, the larger the amount of H_2O_2 added, the lower its oxidation efficiency. The fact that the COD removal rate of EDTA and H_2O_2 oxidation efficiency in the EDTA solution is inversely proportional to the H_2O_2 concentration indicated that an appropriate amount of oxidant should be selected to obtain both a relatively high EDTA removal rate and H_2O_2 oxidation efficiency. The optimal H_2O_2 for this experiment is 40 mmol/L.

Recycling efficiency of the catalyst

In order to investigate the robustness and recyclability of Fe₃O₄ MNPs, the catalyst was recovered magnetically by using an external magnet and washed several times with ethanol and water to remove organic residues before reuse. The reusability of the catalyst was checked by adding fresh precursor (1st run) or used catalysts (2nd–7th runs) in repeated optimum degradation reactions (see Figure 8). From the results of the continuous cycle experiments, it could be seen that Fe₃O₄ MNPs maintained high activity in the five reaction cycles, indicating the good stability of the catalyst for EDTA mineralization. The COD
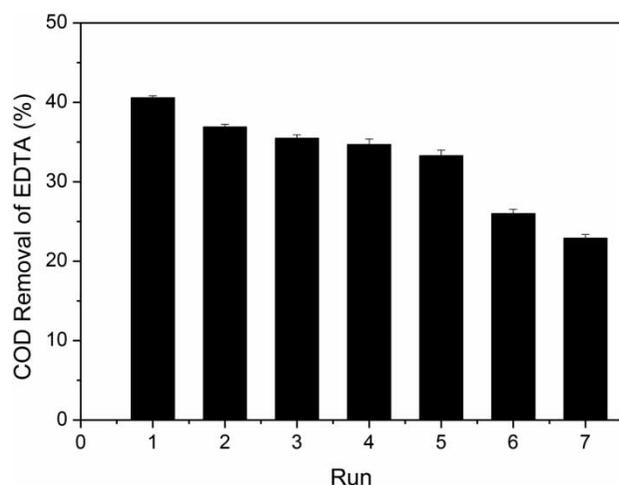
Figure 8 | Consecutive experiments of COD removal with 10 mM Fe_3O_4 MNPs for 4 h (1 g/L $EDTANa_2 \cdot 2H_2O$, 40 mM H_2O_2, pH 7, 303 K).
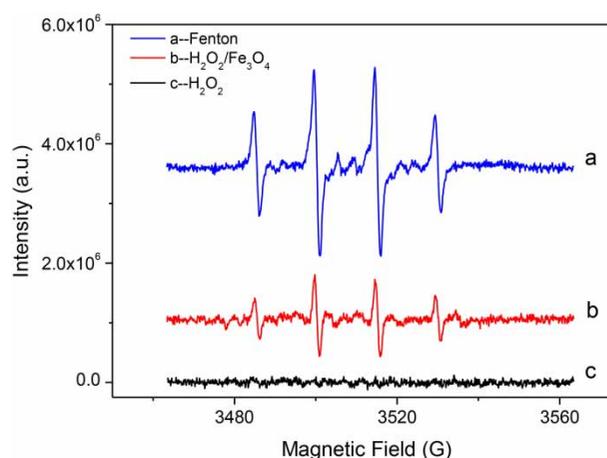

Figure 9 | DMPO spin-trapping ESR spectra. (a) Fenton reaction at pH 3 with H_2O_2 40 mM, Fe^{2+} 4 mM; (b) Fenton-like reaction using Fe_3O_4 MNPs as the catalyst with 40 mM H_2O_2, 10 mM Fe_3O_4 MNPs; (c) reaction with 40 mM H_2O_2.

removal rate of EDTA after five consecutive reaction cycles reached 33.3%, which is slightly lower than the initial run but still significant under neutral pH. However, the COD removal of EDTA decreased sharply to about 26% in the sixth run. This might be caused by two phenomena: (1) after five repeated cycles Fe_3O_4 MNPs were more likely to be oxidized during the treatment process; (2) the active sites on the surface were reduced due to the accumulation of EDTA. These two behaviors would lead to a decrease in the catalytic efficiency of Fe_3O_4 during the sixth or seventh round of mineralization, thereby reducing the COD removal rate of EDTA. In order to avoid perceivable catalytic activity losses, five cycles were selected as the optimal number of cycles to achieve satisfactory COD removal of EDTA.

Mechanism of Fe_3O_4 MNPs catalytic activity

Based on the experimental results, a possible mechanism was discussed according to the nature of the reactive oxygen species (ROS) generated by the decomposition of H_2O_2 catalyzed by Fe_3O_4 MNPs. From the DMPO-based spin trap ESR spectrum, as shown in Figure 9, four peaks in the Fenton reaction system were observed, with a high intensity ratio of 1:2:2:1. These peaks are attributed to a DMPO-OH adduct (Madden & Taniguchi 2001; Li *et al.* 2004). When only H_2O_2 was used in EDTA degradation, no ESR signal was found in the whole reaction. The appearance of characteristic peaks in the ESR spectrum indicates the formation of hydroxyl radicals in the suspension. Although the corresponding radical intensity of H_2O_2/Fe_3O_4 MNPs oxidation system was weaker than that of the Fenton reaction, it can be concluded that HO· radicals

existed in a heterogeneous catalytic oxidation reaction for EDTA degradation and mineralization.

CONCLUSION

Fe_3O_4 MNPs were successfully synthesized using a co-precipitation method that used heterogeneous Fenton-like catalysts to effectively mineralize EDTA from aqueous solution. The morphological characterization of the nanoparticles suggests a quasi-spherical structure with small particle size and a surface area of 49.9 m^2/g. Unlike the traditional Fenton process, the Fe_3O_4 MNPs catalytic system showed high catalytic activity for EDTA mineralization over a pH range of 3.0–9.0. The effect of pH, H_2O_2 concentration, and ferric ion leaching was studied. An optimum catalyst and oxidation agent were necessary to achieve the highest COD removal of EDTA under neutral pH. Moreover, Fe_3O_4 MNPs maintained high catalytic activity after five cycles of continuous degradation of EDTA. ESR measurements confirmed that HO· free radicals, presented in the H_2O_2/Fe_3O_4 MNPs heterogeneous Fenton-like reaction, were the primary active group in the removal of EDTA. These features are beneficial to the application of Fe_3O_4 MNPs towards industrial wastewater treatment.

ACKNOWLEDGEMENTS

DATA AVAILABILITY STATEMENT

All relevant data are included in the paper or its Supplementary Information.

REFERENCES

Amonette, J. E. & Templeton, J. C. 1998 Improvements to the quantitative assay of nonrefractory minerals for Fe (II) and total Fe using 1,10-phenanthroline. *Clays and Clay Minerals* **46**, 51–62.

Bissey, L. L., Smith, J. L. & Watts, R. J. 2006 Soil organic matter–hydrogen peroxide dynamics in the treatment of contaminated soils and groundwater using catalyzed H_2O_2 propagations (modified Fenton's reagent). *Water Research* **40**, 2477–2484.

Chen, L. & Wang, Z. P. 2019 Factors affecting the treatment of refractory organic wastewater using electrochemical advanced oxidation processes. *Applied Chemical Industry* **48** (1), 164–168.

Chiang, K., Lim, T. M., Tsen, L. & Lee, C. C. 2004 Photocatalytic degradation and mineralization of bisphenol A by TiO_2 and platinized TiO_2. *Applied Catalysis A-General* **261**, 225–237.

Gągola, M., Przyjaznyb, A. & Boczkaja, G. 2018 Wastewater treatment by means of advanced oxidation processes based on cavitation – a review. *Chemical Engineering Journal* **338**, 599–627.

Guo, W., Li, Z., Cheng, S., Zhang, Y. & Zhou, X. 2013 Adsorption of EDTA in electroplating wastewater by activated carbon. *Chinese Journal of Environmental Engineering* **7** (10), 4004–4008.

He, J., Yang, X. F., Men, B., Yu, L. & Wang, D. S. 2015 EDTA enhanced heterogeneous Fenton oxidation of dimethyl phthalate catalyzed by Fe_3O_4: kinetics and interface mechanism. *Journal of Molecular Catalysis A-Chemical* **408**, 179–188.

Kanakaraju, D., Glass, B. D. & Oelgemoller, M. 2018 Advanced oxidation process-mediated removal of pharmaceuticals from water: a review. *Journal of Environmental Management* **219**, 189–207.

Kavitha, V. & Palanivelu, K. 2004 The role of ferrous ion in Fenton and photo-Fenton processes for the degradation of phenol. *Chemosphere* **55**, 1235–1243.

Kwan, W. P. & Voelker, B. M. 2003 Rates of hydroxyl radical generation and organiccompound oxidation in mineral-catalyzed Fenton-like systems. *Environmental Science & Technology* **37**, 1150–1158.

Li, L. X., Abe, Y., Kanagawa, K., Usuia, N., Imai, K., Mashinoa, T., Mochizuki, M. & Miyata, N. 2004 Distinguishing the 5,5-dimethyl-1-pyrroline *N*-oxide (DMPO)-OH radical quenching effect from the hydroxyl radical scavenging effect in the ESR spin-trapping method. *Analytica Chimica Acta* **512**, 121–124.

Liu, S. H., Lu, F., Xing, R. M. & Zhu, J. J. 2011 Structural effects of Fe_3O_4 nanocrystals on peroxidase-like activity. *Chemistry-A European Journal* **17**, 620–625.

Lv, A. H., Hu, C., Nie, Y. L. & Qu, J. H. 2012 Catalytic ozonation of toxic pollutants over magnetic cobalt-doped Fe_3O_4 suspensions. *Applied Catalysis B-Environmental* **117–118**, 246–252.

Madden, K. P. & Taniguchi, H. 2001 The role of the DMPO-hydrated electron spin adduct in DMPO-/OH spin trapping. *Free Radical Biology and Medicine* **30**, 1374–1380.

Madden, T. H., Datye, A. K., Fulton, M., Prairie, M. R., Majumdar, S. A. & Stange, B. M. 1997 Oxidation of metal–EDTA complexes by TiO_2 photocatalysis. *Environmental Science & Technology* **31**, 3475–3481.

Massart, R. 1981 Preparation of aqueous magnetic liquids in alkaline and acidic media. *IEEE Transactions on Magnetics* **17**, 1247–1248.

Nascimentoa, U. M., Varandab, L. C. & Azevedoc, E. B. 2019 Preparation, characterization, and catalytic activity of a magnetic photocatalyst (Fe_3O_4@TiO_2). *Desalination and Water Treatment* **150**, 136–145.

Ndjou'ou, A. C., Bou-Nasr, J. & Cassidy, D. 2006 Effect of Fenton reagent dose on coexisting chemical and microbial oxidation in soil. *Environmental Science & Technology* **40**, 2778–2783.

Olive, G., Mercier, A., Moigne, F. L., Rockenbauer, A. & Tordo, P. 2000 2-ethoxycarbonyl-2-methyl-3,4-dihydro-2*H*-pyrrole-1-oxide: evaluation of the spin trapping properties. *Free Radical Biology and Medicine* **28**, 403–408.

Pirkanniemi, K., Metsarinne, S. & Sillanpaa, M. 2007 Degradation of EDTA and novel complexing agents in pulp and paper mill process and waste waters by Fenton's reagent. *Journal of Hazardous Materials* **147**, 556–561.

Sailo, L., Pachuau, L., Yang, J. K., Lee, S. M. & Tiwari, D. 2015 Efficient use of ferrate(VI) for the remediation of wastewater contaminated with metal complexes. *Environmental Engineering Research* **20** (1), 89–97.

Shi, B. F., Zhao, C. C., Ji, Y. J., Shi, J. W. & Yang, H. H. 2020 Promotion effect of PANI on Fe-PANI/Zeolite as an active and recyclable Fenton-like catalyst under near-neutral condition. *Applied Surface Science* **508**, Article Number: 145298.

Sillanpaa, M., Pirkanniemi, K. & Sorokin, A. 2009 Oxidation of EDTA with H_2O_2 catalyzed by Metallophthalocyanines. *Environmental Technology* **14**, 1593–1600.

Wang, M. Q., Wang, N., Tang, H. Q., Cao, M. J., She, Y. B. & Zhu, L. H. 2012 Surface modification of nano- Fe_3O_4 with EDTA and its use in H_2O_2 activation for removing organic pollutants. *Catalysis Science & Technology* **2**, 187–194.

Wang, Y., Gai, L., Ma, W., Jiang, H., Peng, X. & Zhao, L. 2015 Ultrasound-assisted catalytic degradation of methyl orange with Fe_3O_4/Polyaniline in near neutral solution. *Industrial & Engineering Chemistry Research* **54**, 2279–2289.

Wang, N., Jia, D. Q., Jin, Y. Y., Sun, S. P. & Ke, Q. 2017 Enhanced Fenton-like degradation of TCE in sand suspensions with magnetite by NTA/EDTA at circumneutral pH. *Environmental Science and Pollution Research* **24** (21), 17598–17605.

Wang, H. J., Zhao, Z. L., Zhang, X. S., Dong, W. Y., Cao, Z., He, L. & Wang, X. 2020 Rapid decomplexation of Ni-EDTA by microwave-assisted Fenton reaction. *Chemical Engineering Journal* **381**, Article Number: UNSP 122703.

Wardas, W. & Lebek, J. 1998 EDTA and Fe(III)-EDTA adsorption on post-vanillin lignin during its precipitation. *Cellulose Chemistry and Technology* **32** (3–4), 269–277.

Xia, F. & Nan, Z. D. 2020 Excellent Fenton-like catalyst application in alkaline solution. *Functional Materials Letters* **13** (2), Article Number: 2050002.

Yang, C., Xu, Y. R., Teo, K. C., Goh, N. K., Chia, L. S. & Xie, R. J. 2005 Destruction of organic pollutants in reusable wastewater using advanced oxidation technology. *Chemosphere* **59**, 441–445.

Yang, S. T., Zhang, W., Xie, J., Liao, R., Zhang, X., Yu, B., Wu, R., Liu, X. G., Li, H. & Guo, Z. 2015 $Fe_3O_4@SiO_2$ nanoparticles as a high-performance Fenton-like catalyst in a neutral environment. *RSC Advances* **5**, 5458–5463.

Zárate-Guzmán, A. I., González-Gutiérrez, L. V., Godínez, L. A., Medel-Reyes, A., Carrasco-Marín, F. & Romero-Cano, L. A. 2019 Towards understanding of heterogeneous Fenton reaction using carbon-Fe catalysts coupled to in-situ H_2O_2 electro-generation as clean technology for wastewater treatment. *Chemosphere* **224**, 698–706.

Zeng, Y., Hao, R., Xing, B. G., Hou, Y. L. & Xu, Z. C. 2010 One-pot synthesis of Fe_3O_4 nanoprisms with controlled electrochemical properties. *Catalysis Communications* **46**, 3920–3922.

Zhang, S. X., Zhao, X. L., Niu, H. Y., Shi, Y. L., Cai, Y. Q. & Jiang, G. B. 2009 Superparamagentic Fe_3O_4 nanoparticles as catalysts for the catalytic oxidation of phenolic and aniline compounds. *Journal of Hazardous Materials* **167**, 560–566.

Zhang, M. H., Dong, H., Zhao, L., Wang, D. X. & Meng, D. 2019 Wastewater treatment based on optimization perspective. *Science of the Total Environment* **670** (20), 110–121.

Zhu, Y. P., Zhu, R. L., Xi, Y. F., Zhu, J. X., Zhu, G. Q. & He, H. P. 2019 Strategies for enhancing the heterogeneous Fenton catalytic reactivity: a review. *Applied Catalysis B-Environmental* **255**, 117739.